

See discussions, stats, and author profiles for this publication at: <https://www.researchgate.net/publication/233209613>

Geochemical constraints on the origin and environment of Lower Cambrian, selenium-rich siliceous sedimentary rocks in the...

Article in *International Geology Review* · May 2012

DOI: 10.1080/00206814.2011.580625

CITATIONS

5

READS

149

6 authors, including:



Feng Caixia

Chinese Academy of Sciences

38 PUBLICATIONS 638 CITATIONS

[SEE PROFILE](#)



Guoxiang Chi

University of Regina

129 PUBLICATIONS 1,210 CITATIONS

[SEE PROFILE](#)



Jiajun Liu

China University of Geosciences (Beijing)

173 PUBLICATIONS 1,209 CITATIONS

[SEE PROFILE](#)



Ian M. Coulson

University of Regina

69 PUBLICATIONS 984 CITATIONS

[SEE PROFILE](#)

Some of the authors of this publication are also working on these related projects:



Geochronological, geochemical and fluid-inclusion investigation of the Maw REE Zone prospect and its potential relationship with unconformity-type uranium mineralization in the Wheeler River area, Athabasca basin, Saskatchewan. [View project](#)



Barium deposit research [View project](#)

This article was downloaded by: [University of Regina]

On: 27 March 2012, At: 10:50

Publisher: Taylor & Francis

Informa Ltd Registered in England and Wales Registered Number: 1072954 Registered office: Mortimer House, 37-41 Mortimer Street, London W1T 3JH, UK



International Geology Review

Publication details, including instructions for authors and subscription information:

<http://www.tandfonline.com/loi/tigr20>

Geochemical constraints on the origin and environment of Lower Cambrian, selenium-rich siliceous sedimentary rocks in the Ziyang area, Daba region, central China

Caixia Feng ^a, Guoxiang Chi ^b, Jiajun Liu ^c, Ruizhong Hu ^a, Shen Liu ^a & Ian M. Coulson ^b

^a The State Key Laboratory of Ore Deposit Geochemistry, Institute of Geochemistry, Chinese Academy of Sciences, Guiyang, 550002, PR China

^b Department of Geology, University of Regina, Regina, Saskatchewan, Canada, S4S 0A2

^c China University of Geosciences, Beijing, 100083, PR China

Available online: 09 Jun 2011

To cite this article: Caixia Feng, Guoxiang Chi, Jiajun Liu, Ruizhong Hu, Shen Liu & Ian M. Coulson (2012): Geochemical constraints on the origin and environment of Lower Cambrian, selenium-rich siliceous sedimentary rocks in the Ziyang area, Daba region, central China, *International Geology Review*, 54:7, 765-778

To link to this article: <http://dx.doi.org/10.1080/00206814.2011.580625>

PLEASE SCROLL DOWN FOR ARTICLE

Full terms and conditions of use: <http://www.tandfonline.com/page/terms-and-conditions>

This article may be used for research, teaching, and private study purposes. Any substantial or systematic reproduction, redistribution, reselling, loan, sub-licensing, systematic supply, or distribution in any form to anyone is expressly forbidden.

The publisher does not give any warranty express or implied or make any representation that the contents will be complete or accurate or up to date. The accuracy of any instructions, formulae, and drug doses should be independently verified with primary sources. The publisher shall not be liable for any loss, actions, claims, proceedings, demand, or costs or damages whatsoever or howsoever caused arising directly or indirectly in connection with or arising out of the use of this material.

Geochemical constraints on the origin and environment of Lower Cambrian, selenium-rich siliceous sedimentary rocks in the Ziyang area, Daba region, central China

Caixia Feng^{a*}, Guoxiang Chi^b, Jiajun Liu^c, Ruizhong Hu^a, Shen Liu^a and Ian M. Coulson^b

^aThe State Key Laboratory of Ore Deposit Geochemistry, Institute of Geochemistry, Chinese Academy of Sciences, Guiyang 550002, PR China; ^bDepartment of Geology, University of Regina, Regina, Saskatchewan, Canada S4S 0A2; ^cChina University of Geosciences, Beijing 100083, PR China

The Ziyang area is one of the two major regions of central China subjected to selenium (Se) poisoning. Systematic studies of Se contents of different lithologies from this area indicate that Lower Cambrian, carbonaceous, and siliceous strata host the highest Se contents (with Se contents of up to 278 ppm). We have investigated their geochemical characteristics (major and trace elements, and Si and O isotopes), origin, and sedimentary environment of formation. The siliceous rocks are characterized by a wide range in major elements, and are enriched in Se, Ba, Cu, Ni, V, As, Sb, and U relative to average continental crust. They are also enriched in light rare earth elements relative to heavy rare earth elements ($La_N/Yb_N = 1.64\text{--}35.7$) and show weak or moderate negative Ce anomalies and strong positive Eu anomalies. $\delta^{30}Si_{NBS-28}$ and $\delta^{18}O_{V-SMOW}$ values range from -0.3‰ to 0.6‰ and 16.1‰ to 21.7‰ , respectively. The homogenization temperatures of inclusions within the studied samples range from 113°C to 319°C , and their salinities from 1.2 to 13.7 wt.% NaCl equivalent. Our results suggest that the studied siliceous rocks resulted from hydrothermal sedimentation in a relatively anoxic semi-deep sea sedimentary environment. The hydrothermal fluid responsible for Se-mineralization involved the mixing of low-temperature high-salinity fluid, low-temperature low-salinity fluid, and a high-temperature low-salinity basinal fluid in the NaCl–(KCl)–H₂O system.

Keywords: siliceous rocks; selenium content; sedimentary environment; Shaanxi Province, China

Introduction

The element selenium (Se) occurs in low concentrations in both the Earth's crust and mantle (~ 0.05 ppm) (Liu *et al.* 1984), and is considered to be mainly dispersed as sulphides formed through hypogene processes (D'yachkova and Khodakovskiy 1968; Simon *et al.* 1997). Several studies report the discovery of selenium minerals in a variety of mineralized occurrences, such as epithermal-, skarn-, sandstone-, and unconformity-type uranium deposits (Simon and Essene 1996; Simon *et al.* 1997; Förster and Tischendorf 2001). In China, Se has also been reported to be highly enriched in the 'black rock series', such as the Lower Cambrian black shale of Zunyi, Guizhou Province (Fan 1983; Coveney *et al.* 1994; Luo *et al.* 2004; Orberger *et al.* 2007), and the Cambrian siliceous rocks of Ziyang, Shaanxi Province (Mei 1985; Luo *et al.* 2001, 2004, Feng *et al.* 2004, 2007a). Many important, individual Se deposits have been described within these strata, for example, the La'erma-Qiongmo Au–Se deposit at West Qinling Mountain (Wen and Qiu 1999; Liu *et al.* 2000) and the Yutangba Se deposit in Enshi, Hubei Province (Song 1989; Wang and Li 1996; Yao *et al.* 2002; Zhu 2000; Feng *et al.* 2002, 2004, 2007b). In the bulk of these studies, Se is enriched in siliciclastic-dominated lithologies. As such,

to better constrain the source of Se in these deposits it is important to understand not only the origins of the siliceous rocks but also the sedimentary environment in which they formed.

Since the discovery, in the 1960s, of severe Se-poisoning in the inhabitants of the town of Shuang'an, in the Ziyang area, Shaanxi Province of central China (Figure 1; Mei 1985), numerous studies have been conducted locally to determine the abundance, source, and origin of Se (Li *et al.* 1982, 2000; Mei 1985; Zhao *et al.* 1993; Luo *et al.* 2001, 2004). The results of these investigations point to Se derivation mainly from Se-rich coal-bearing and carbonaceous strata (Mei 1985; Luo *et al.* 2001). Based upon systematic geochemical analyses of all rock types occurring in this region, siliceous rocks have the highest Se contents of any studied lithologies (Feng 2004). The origin of these siliceous rocks and their sedimentary environment of formation remain to be determined and represent the focus of this article.

The significance of understanding the origin of the siliceous rocks present in the Ziyang study area extends beyond identifying the source of the poisonous Se and delineating its distribution. Selenium-rich siliceous rocks form part of the Lower Cambrian 'black rock series', which

*Corresponding author. Email: fengcaixia@vip.gyig.ac.cn

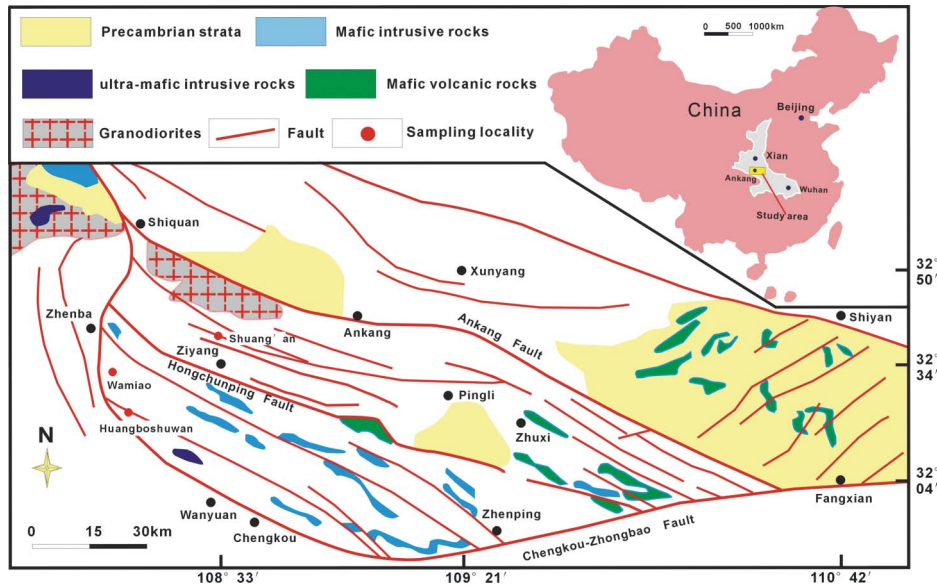


Figure 1. Geological map of the Ziyang area, Daba region, China (after BGMRS 1982; Luo 2006). The insert map shows the location of the study region in China.

are widely distributed in the Yangtze and Tarim cratons in southern and western China. The ‘black rock series’ comprises black carbonaceous shale, black carbonaceous argillo-siliceous rocks, black carbonaceous chert, and carbonaceous argillaceous siltstone (Fan *et al.* 1984; Chen 1990; Li and Gao 1996; 2000; Yu and Qiu 1998; Steiner *et al.* 2001; Mao *et al.* 2002; Yu *et al.* 2002; Orberger *et al.* 2007; Feng *et al.* 2010). Besides Se, this series also contains important occurrences of Cu, Pb, Zn, As, Ni, S, Ag, U, Mn, and platinum group elements (PGE) (Kucha and Pawlowski 1986; Püttmann *et al.* 1988; Sawlowicz 1989; Grauch *et al.* 1991; Coveney *et al.* 1992; Hulbert *et al.* 1992; Pasava 1993; Sun and Püttmann 1997; Mossman *et al.* 2005; Polgary *et al.* 2006; Orberger *et al.* 2007). Moreover, the ‘black rock series’ at the base of the Cambrian have a widespread (virtually global) occurrence and they carry important information concerning the formation and tectonic history of sedimentary basins (Yu *et al.* 2009). A study of the origin of these siliceous rocks will, therefore, help in our overall understanding of the mechanisms of enrichment of Se and perhaps other metals found within the ‘black rock series’.

We now investigate the origin and sedimentary environments where these siliceous rocks were deposited, based on interpretations of the data for elementary geochemistry (major and trace elements), fluid inclusion, and Si-, O-isotopes. The evolution of ore-forming fluid and Se (and other metals) enrichment mechanisms in the Lower Cambrian ‘black rock series’ are also discussed.











Geological setting

The study area is located in the Daba region of central China (Figure 1). Geologically, it is located in the transition zone between the northern margin of the Yangtze Craton and the southern margin of the Qinling Orogenic Belt. Here, Cambrian strata are cut by a series of NW-trending faults, including the Chengkou-Zhongbao Fault, Hongchunba-Zengjiaba Fault, and the Ankang Fault (Bureau of Geology and Mineral Resources of Shaanxi Province 1982; Figure 1). In the Daba region, Neoproterozoic and early Palaeozoic strata, including carbonates, siliceous-carbonaceous shale, and siliciclastics, are interbedded with and intruded by volcanic rocks (dolerite, trachy-dolerite, trachyte, and volcanic tuff). Faulting and folding complicate the geological structure (Luo *et al.* 2004). The Cambrian strata, which unconformably overlie Neoproterozoic (Sinian) limestones, consist of the Lujiaping and Jianzhuba formations (Table 1). Siliceous rocks occur throughout the two formations, interbedded with limestone, dolomite, siltstone, carbonaceous slate, and coal (Table 1). The Se-mineralized siliceous rocks are stratiform and lensoid, and vary from thick- to thinly bedded (Figure 2).

Samples and analytical methods

Samples of siliceous rocks were collected from the Shuang’an, Wamiao, and Huangboshuwan areas (Figure 1). Quartzite samples were selected following binocular microscope examination. In addition, a quartz

Table 1. The Lower Cambrian strata of the Ziyang area, Daba region, China (after Bureau of Geology and Mineral Resources of Shaanxi Province 1982).

Stratum	Thickness (m)		Rock types and their relation
Jianzhuba Formation	185.9		Dark-grey to greyish black limestones interbedded with siliceous rocks or stone coal
Lujiaping Formation	51.5		Black carbonaceous siliceous slates and thin-layered carbonaceous mudstone interbeds in the middle and upper parts
	35.5		Greyish-black to black carboniferous slates, occasionally interbedded with carbonaceous siltstone, with siderite nodules and limestone observed at the bottom
	30.7		Poor-quality stone coal including siderite nodules intercalated with slate in the upper part and siderite nodules in the lower part
	49.8		Dark grey slate intercalated with grey limestone in the middle and upper parts, with siderite nodules in the lower part
	24.9		Black massive siliceous rocks with thin-moderately thick thickness, intercalated with two layers of dark grey P-bearing limestone in the lower part
	20.1		Light grey massive P-bearing dolomite with pyrite in the upper and middle parts, also intercalated with one layer of brecciated siliceous rocks
	57.7		Limestone, siliceous slate and poor-quality stone coal, siderite nodules in the upper part; dark grey thick-layered P-bearing limestone intercalated with siliceous nodule in the middle and lower parts
Conformity	60.7		Black massive siliceous rocks, intercalated with P-bearing calcaceous siltstone in the lower part, and P-bearing siliceous rocks at the bottom
Underlying strata	Upper Sinian grey P-bearing siliceous limestone and siliceous banded limestone		

vein present at Shuang'an was also sampled for study. Whole-rock samples were trimmed to remove weathered surfaces, cleaned with de-ionized water, and crushed and powdered with an agate mill. The powdered samples were analysed for Se, major elements, trace elements, and Si and O isotopes. Doubly polished thick sections of quartz, barite, and witherite were also prepared from selected samples and examined by standard microscopy before undertaking further analyses.

The Se contents of the samples were determined by fluorospectrometry (utilizing a Shimadzu RF-540 fluorescence detector) and ultraviolet spectrophotometry (using a Shimadzu UV-300 spectrophotometer) analysis at the State Key Laboratory of Ore Deposit Geochemistry, Institute of Geochemistry, Chinese Academy of Sciences (IGCAS). The procedures for sample dissolution and calibration with international rock standards have been documented by Zhu (2000) to which the reader is referred.

Major elements were analysed by X-ray fluorescence spectrometry (at IGCAS, with analytical uncertainties varying from 1% to 3%). Loss on ignition was obtained using 1.0 g of powdered sample heated up to 1100°C for 1 hour. Ferrous oxide (FeO) content was determined by wet chemical methods. Trace elements were analysed with an element ICP-MS at IGCAS. The procedures for sample dissolution and calibration by reference to international rock standards are documented in Qi *et al.*

(2000). Analytical discrepancy is less than 5% for all elements, and analytical results of international standards OU-6 and GBPG-1 are in agreement with recommended values.

Silicon and oxygen isotopes were analysed using the SiF₄ and BrF₅ methods with a MAT-251 mass spectrometer at the Institute of Mineral Resources, Chinese Academy of Geological Sciences. $\delta^{30}\text{Si}$ and $\delta^{18}\text{O}$ are expressed relative to the NBS-28 and Vienna Standard Mean Ocean Water, respectively. The analytical precision is $\pm 0.1\%$ and $\pm 0.2\%$ for $\delta^{30}\text{Si}$ and $\delta^{18}\text{O}$, respectively. For the O and Si isotopic analysis, the analytical procedures are described in Clayton and Mayeda (1963) and Li *et al.* (1995).

Microthermometric studies were carried out at the fluid inclusion laboratory, IGCAS, following the procedures outlined by Roedder (1984) and Shepherd *et al.* (1985), utilizing a Linkam THMGS600 heating-freezing stage. The stage was calibrated against pure H₂O synthetic inclusions (0 and +374.1°C) and with pure CO₂-bearing natural inclusions (-56.6°C). Measurements below 0°C are accurate to $\pm 0.1^\circ\text{C}$, whereas in heating runs, temperatures are accurate to $\pm 1^\circ\text{C}$. Salinity (expressed as wt.% NaCl equivalent) data were calculated by reducing raw thermometric data with the program of Chi and Ni (2007). Thirty freezing-temperature and 30 homogenization-temperature data sets have been obtained, including those from this study and other data from recent research.

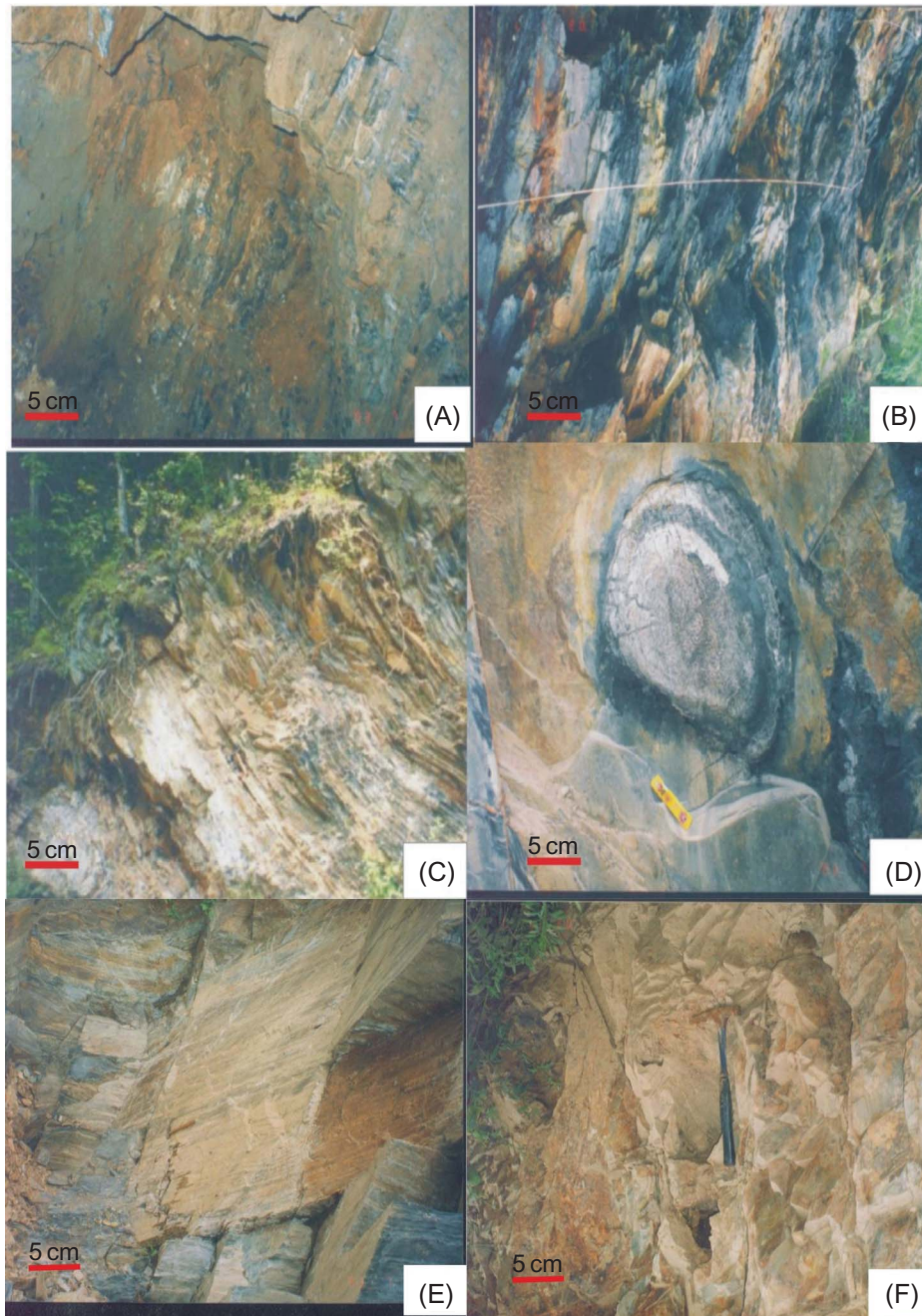


Figure 2. Different types of siliceous rocks encountered in the Lower Cambrian Luojiaping Formation of the Ziyang area, Shaanxi Province, China. (A) Bedded siliceous rock; (B) carbonaceous siliceous rock; (C) muddy siliceous rock; (D) pyrite-rich siliceous rock; (E) the sampling site of S-1 (siliceous rock interbedded with muddy rock, with low organic matter contents); (F) the sampling site of S-7 (siliceous rock, with low organic matter contents).

Results

Selenium contents

The Se contents of analysed samples are presented in Table 2; they show a wide range from 8.1 (WM-20, carbonaceous siliceous slate) to 278 ppm (W-7, carbonaceous siliceous rock). Siliceous rocks are the dominant Se-rich lithology, although Se is also high in coal. Because of the

organic affinity of the disperse element Se, its concentration in a rock increases proportionately to the content of organic carbon (Song 1989; Luo and Jiang 1995; Kirst and Timo 1996; Wen 1999). In this article, two siliceous samples (S-1 and S-7) with relatively low Se contents likely reflect their low organic carbon content, as can be seen in Figure 2E and 2F.

Table 2. Selenium content (ppm) in different types of rock of the Lujiaping Formation from the Ziyang area, Daba region, China.

Sample	Locality	Rock type	Se	Sample	Locality	Rock type	Se
HB-3	Huangboshuwan	Siliceous rock	20.9	S-1	Shuang'an	Siliceous rock	12.9
HB-5	Huangboshuwan	Siliceous rock	50.9	S-7	Shuang'an	Siliceous rock	15.1
HB-10	Huangboshuwan	Siliceous rock	23.8	S-36	Shuang'an	Py-bearing mud rock	28.4
S-41	Shuang'an	Carbonaceous siliceous rock	260	S-38	Shuang'an	Mud rock	32.5
S-29	Shuang'an	Carbonaceous siliceous rock	278	S-45	Shuang'an	Carbonaceous slate	21
WM-7	Wamiao	Py-bearing siliceous rock	110.3	WM-11	Wamiao	Mud siliceous rock	22.9
WM-19	Wamiao	coal stone	43.7	WM-20	Wamiao	Carbonaceous siliceous slate	8.13
Sample GBW07107	Rock type shale	Se(MV*)(ppm)(n = 3) 0.082 ± 0.003	Se(RV*)(ppm) 0.078 ± 0.002	Sample GBW07105	Rock type Olivine basalt	Se(MV*)(ppm)(n = 3) 0.072 ± 0.005	Se(RV*)(ppm) 0.073 ± 0.003

Note: RV*: recommended value; MV*: measured value.

Major elements

The analytical results for major elements of the samples (Table 3) indicate a wide range in chemical compositions, with SiO₂ varying from 63.62 wt.% to 95.24 wt.% (average 82 wt.%), TiO₂ from 0.0001 wt.% to 0.47 wt.%, Al₂O₃ from 0.09 wt.% to 0.68 wt.%, Fe₂O₃ from 0.48 wt.% to 6.05 wt.%, FeO from 0.12 wt.% to 1.25 wt.%, CaO from 0.6 wt.% to 2.9 wt.%, Na₂O from 0.04 wt.% to 0.39 wt.%, K₂O from 0.02 wt.% to 1.56 wt.%, and P₂O₅ from 0.001 wt.% to 2.27 wt.%. MnO and MgO contents are relatively constant, varying from 0.04 wt.% to 0.15 wt.% and 0.1 wt.% to 0.4 wt.%, respectively.

Trace elements

The analytical results for trace elements are shown in Table 4. The siliceous rocks have higher Se, Ba, As, Sb, V, Cu, U, and Sr contents than is typical for the crust, with average enrichment coefficients of 1863, 129, 35.4, 18.0, 9.65, 2.66, 4.21, and 2.00, respectively. In contrast, Co, Ni, Zr, and Th contents are lower than the averages in the crust (Li 1992) (Table 4).

Relative to a C1-chondrite, the Ziyang siliceous rocks are all characterized by slight light rare earth element enrichment relative to heavy rare earth elements, with a wide range of La_N/Yb_N values (1.64–35.7), moderate to small negative Ce anomalies (Ce/Ce* = 0.22–0.91) and moderate to large positive Eu anomalies (Eu/Eu* = 1.14–10.3), except for two samples (Eu/Eu* = 0.96–0.97) (Figure 3).

Si and O isotopes

The δ³⁰Si values of the siliceous rocks and quartz range from –0.3‰ to 0.6‰ (Table 5, Figure 4A). The δ¹⁸O values vary from 16.1‰ to 21.7‰ (Table 5, Figure 4B).

Fluid inclusion microthermometry

Inclusion type

Based on the number of phases observed at room temperature, filling degree, and phase variations during heating and freezing experiments, three fluid inclusion types are identified. Type-I fluid inclusions contain H₂O liquid and vapour. Type-I fluid inclusions show irregular, rounded, or rectangular shape, and are the dominant type in our samples. They can occur randomly distributed, clustered in the centres of grains, or as pseudosecondary trails. Their size range is from ~5 μm to 15 μm. The volumetric proportion of the vapour phase varies from 20 vol.% to 70 vol.% (Figure 5A and 5B). Type-II fluid inclusions contain H₂O liquid only (L). Type-II inclusions generally show irregular forms, range in size from ~5 μm to 15 μm and are isolated (primary), or less commonly occur as pseudosecondary trails (Figure 5A). Type-III fluid inclusions contain pure vapour C_mH_n. These inclusions occur rarely and range in diameter from 12 μm to 20 μm. Their shape varies from irregular to ellipsoidal (Figure 5B).

The host minerals of the fluid inclusion are quartz, barite, and witherite. Fluid inclusion assemblages comprising Type-I, -II, and -III inclusions within the same cluster or trail are common, as are Type-I inclusions with variable proportions of liquid and vapour of H₂O. Daughter minerals have not been found in any of the fluid inclusions observed.

Homogenization temperature and salinity

In addition to our own work, we have compiled homogenization temperatures and salinity data for samples of quartz, barite, and witherite from previous studies (Duan 1999; Liu *et al.* 2010). Homogenization temperatures range from 113°C to 319°C (Table 6). The average homogenization temperatures are 168°C in quartz, 145°C in barite, and 137°C in witherite. Four homogenization temperature

Table 3. The chemical composition (wt.%) of Lower Cambrian siliceous rocks from the Ziyang area, Daba region, China.

Sample	S-1	S-4	S-7	WM-11	HB-3	HB-5	S-41	S-29	Average value
SiO ₂	94.79	95.24	92.97	72.93	72.83	73.67	63.62	89.94	82
TiO ₂	0.0001	0.002	0.001	0.34	0.2	0.47	0.22	0.12	0.17
Al ₂ O ₃	0.3	0.3	0.3	0.61	0.18	0.2	0.09	0.68	0.33
Fe ₂ O ₃	0.67	0.6	0.7	0.87	0.71	6.05	0.48	0.73	1.35
FeO	0.2	0.21	0.36	0.5	0.3	1.25	0.2	0.15	0.4
MnO	0.04	0.07	0.15	0.06	0.1	0.11	0.07	0.07	0.08
MgO	0.28	0.11	0.33	0.29	0.4	0.8	0.1	0.11	0.3
CaO	1.84	1.54	1.87	1.26	1	2.9	0.6	2.7	1.71
Na ₂ O	0.22	0.29	0.26	0.39	0.06	0.1	0.04	0.05	0.18
K ₂ O	0.08	0.14	0.09	1.56	0.03	0.95	0.02	0.04	0.36
LOI	1.2	1.1	1.96	8.87	3.2	12.6	1.58	2.35	4.11
P ₂ O ₅	0.2	0.2	0.23	0.2	0.003	0.2	0.001	2.27	0.41
BaCO ₃				11.5	20.73		32.63		
Total	99.82	99.8	99.22	99.38	99.73	99.3	99.65	99.21	99.51
Al/(Al+Fe+Mn)	0.195	0.200	0.152	0.655	0.106	0.020	0.081	0.345	0.18
SiO ₂ /MgO	338.54	856.82	281.73	251.48	182.08	92.09	636.20	817.64	273.33

Note: LOI = loss on ignition.

Table 4. The contents of trace and REE elements (ppm) in the Lower Cambrian siliceous rocks from the Ziyang area, Daba region, China.

Sample	S-1	S-4	S-7	WM-11	HB-3	HB-5	S-41	S-29	A	B	C
Co	1.91	1.42	2.73	1.48	4.40	6.46	2.22	1.94	2.82	15	0.19
Ni	14.7	8.19	25.2	28.1	33.6	217	26.6	33.4	48.4	56	0.86
Cu	101	80.4	54.7	27.7	99.1	222	162	105	107	40	2.66
Cr	32.0	33.3	36.2	106	42.8	298	53	96.7	87.3	63	1.39
Zr	9.33	31.3	18.9	82.5	5.66	87.8	5.35	23.9	33.1	132	0.25
Sb	3.8	2.31	5.19	12.8	2.77	108	4.34	4.54	18.0	1	18
As	947	699	744	39.8	9.59	68	31.9	11.2	319	9	35.4
Sr	17.5	9.39	31.7	203	2464	490	2727	617	820	410	2
Ba	537	1091	1344	45614	148369	57641	241907	59667	69521	538	129
V	44.2	245	112	1813	242	3727	329	438	869	90	9.65
Y	7.12	20.7	8.83	43.3	10.5	135	22.5	76.2	40.5	32	1.26
Th	0.42	0.78	0.41	6.5	0.2	3.93	0.18	0.98	1.68	8.5	0.2
U	6.83	3.14	6.7	16.5	15.3	23.5	5.95	14.5	11.5	2.8	4.12
Hf	0.32	0.57	0.28	2.61	0.14	1.58	0.11	0.42	0.75		
Ta	0.02	0.02	0.02	0.52	0.02	0.3	0.04	0.15	0.14		
La	2.95	2.91	2.03	30.7	18.2	46.6	18.8	26.7			
Ce	3.53	4.16	3.60	48.1	6.83	35.7	5.33	28.9			
Pr	0.65	0.68	0.47	6.08	1.22	10.7	1.96	7.51			
Nd	2.80	3.38	1.98	23.1	3.20	47.6	8.49	32.6			
Sm	0.49	0.85	0.41	4.27	1.14	10.9	2.30	8.35			
Eu	0.25	0.38	0.34	2.02	3.35	3.96	*	2.94			
Gd	0.52	1.21	0.60	4.39	0.87	14.5	2.33	10.3			
Tb	0.07	0.21	0.10	0.70	0.16	2.32	0.35	1.7			
Dy	0.61	1.42	0.86	5.19	1.00	17.3	2.06	11.6			
Ho	0.15	0.36	0.19	1.18	0.22	3.91	0.54	2.50			
Er	0.54	1.31	0.63	3.75	0.60	13.3	1.72	7.80			
Tm	0.08	0.18	0.09	0.49	0.08	1.95	0.26	1.10			
Yb	0.59	1.27	0.65	3.07	0.37	12.9	1.63	7.41			
Lu	0.10	0.22	0.12	0.40	0.05	1.95	0.28	1.00			
(La/Yb) N	3.56	1.64	2.23	7.15	35.7	2.59	8.27	2.58			
LREE	10.7	12.3	8.74	91.2	30.7	156	28.4	74.4			
HREE	2.66	6.18	3.24	19.2	3.32	56.7	9.17	43.4			
$\sum_{\delta Ce}^{REE}$	13.3	18.5	12.0	110	34.0	212	37.5	118			
δEu	0.63	0.73	0.91	0.86	0.36	0.39	0.22	0.50			
δEu	1.50	1.14	2.11	1.43	10.29	0.96	*	0.97			

Notes: N-chondrite normalised, C1-chondrite values are from Sun and McDonough (1989).

A: average value; B: the element abundance in crust (Li, 1992); C: enrichment coefficient (A/B).

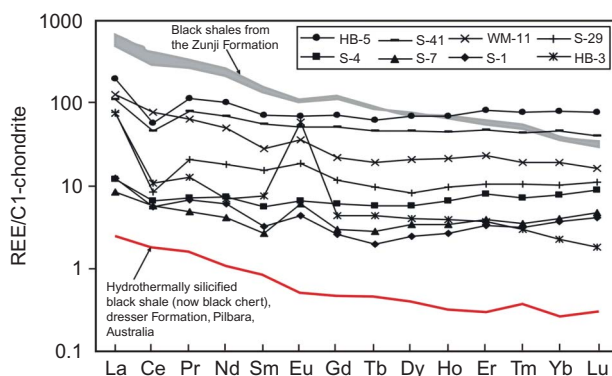


Figure 3. Chondrite(C1)-normalized rare earth element (REE) diagrams for the Lower Cambrian siliceous rocks of the Ziyang area. C1 values are from Sun and McDonough (1989). Data for the black shales from the Zunji Formation and the hydrothermally silicified black shale (now black chert) of the Dresser Formation, Pilbara, Australia, are from Orberger *et al.* (2007).

peaks are revealed in the stacked histogram (Figure 6A), that is, a peak at 110–130°C, mainly consisting of inclusions within barite and witherite, a 140–170°C peak for inclusions in quartz and calcite, a 180–220°C peak for inclusions in quartz and barite, and further, a 260–300°C peak exhibited in inclusions just in quartz.

The first melting temperatures of the aqueous fluid inclusions range from –17°C to –23°C, suggesting that these can be modelled in the NaCl–(KCl)–H₂O system. Salinities range from 1.2 wt.% to 13.7 wt.% NaCl equivalent (Table 6), with a mode around 2–5 wt.% NaCl equivalent (Figure 6B). The average salinity for fluid inclusions in quartz is 3.3 wt.% NaCl equivalent, 5.0 wt.% in barite, and 7.9 wt.% in witherite. The difference in salinity between the various minerals is evident in Figure 6B.

The negative Th-salinity trend of quartz, barite, and witherite probably resulted from a low-temperature high-salinity fluid during the earlier stage of mineralization.

Table 5. The Si and O isotopic compositions (‰) of Lower Cambrian siliceous rocks from the Ziyang area, Daba region, China.

Sample	HB-5	S-41	S-29	WM-11	Quartz1	Quartz2	Quartz3	WM-12	WM-17
Locality	Huangboshuwan	Shuang'an	Shuang'an	Wamiao	Shuang'an	Shuang'an	Shuang'an	Wamiao	Wamiao
$\delta^{18}\text{O}_{\text{SMOW}}$	20.5	19.1	20	18.6	17.8	16.5	16.1	20.7	21.7
$\delta^{30}\text{Si}_{\text{NBS-28}}$	-0.1	-0.3	-0.2	-0.2	0.3	0.4	0.5	0.4	0.6

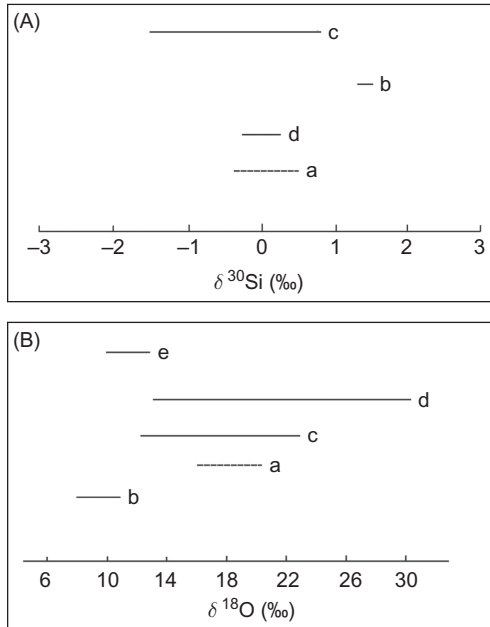


Figure 4. (A) Plot highlighting the distribution of $\delta^{30}\text{Si}$ values for quartz and siliceous rocks of various origins (after Douthitt 1982; Clayton 1986). a, Siliceous rocks from the Ziyang area; b, quartz from groundwater; c, quartz from hot water; d, soluble silica from a hot spring. (B) Plot highlighting the range in $\delta^{18}\text{O}$ values for quartz of various origin (after Clayton 1986). a, siliceous rocks from the Ziyang area; b, igneous quartz; c, hot-spring-type quartz; d, diagenetic quartz; e, quartz beach-sand.

Then the mixing of low-temperature low-salinity fluid with high-temperature low-salinity fluid in quartz, barite, and witherite occurred in the main stage of mineralization (Figure 7).

Data interpretation and discussion

Genesis of the siliceous rocks

Siliceous rocks may form as the result of biochemical sedimentation, diagenesis, hydrothermal venting in a sub-aqueous environment, and hydrothermal alteration in various environments (Rona 1978; Adachi *et al.* 1986; Yamamoto 1987; Feng and Liu 2001; Qi *et al.* 2003; Yang *et al.* 2006). Based on the bedded occurrence of the siliceous rocks in the study area, they most likely formed within a sedimentary basin. The lack of biogenetic textures and geochemical characteristics, as discussed below, strongly suggest that the siliceous rocks were formed from chemical sedimentation from vented hydrothermal fluids.

Siliceous rocks of a hydrothermal origin have relatively lower Mg and Al and high Fe and Mn contents compared to non-hydrothermal origin siliceous rocks (Yamamoto 1987). For example, MgO has been found to be depleted in mid-ocean ridge hydrothermal systems; in hydrothermal fluids (350°C) taken from the East Pacific Rise mid-ocean ridge, the MgO content is near zero (Edmond and Damm 1983). The MgO contents in our siliceous samples are mostly

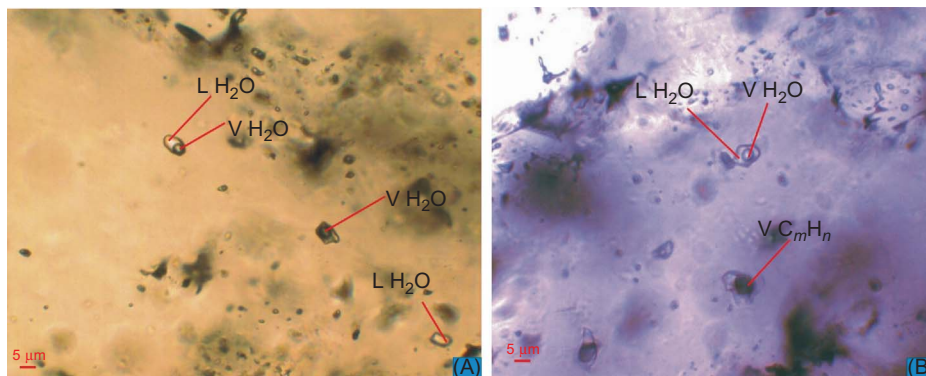


Figure 5. Photomicrographs of fluid inclusions identified in various lithologies from the Ziyang area, Daba region, China: (A) Type-I and Type-II fluid inclusions (including pseudosecondary fluid inclusions) with different L/V ratios in quartz; (B) Type-I and Type-III fluid inclusions with different L/V ratios in barite. L, liquid, V, vapour.

Table 6. Homogenization temperature and salinity of fluid inclusion in rocks from the Ziyang area, Daba region, China.

Sample	Ore block	Minerals	Size	V/L	Tm-ice(°C)	Th(°C)	Slt (wt.% NaCl eq.)			
S-41	Shuang'an	Quartz	12~15	25	-1.1	319	1.85			
			12	30	-0.8	307	1.35			
			12	25	-1.6	126	2.7			
			11	30	-1.4	135	2.35			
			10	9	-1.9	156	3.18			
			8	12	-1.6	126	2.7			
HB-9	Huangboshuwan	Quartz	10	5	-0.7	173	1.2			
HB-9-e	Huangboshuwan	Quartz	10	5	-1.1	255	1.85			
S-39a	Shuang'an	Quartz	5~6	7	-1.3	147	2.2			
			6~7	10	-1.9	156	3.18			
HB-1	Huangboshuwan	Barite	5	7	-0.5	113	0.85			
			8	10	-1.2	120	2.05			
WM-2	Wamiao	Witherite	4~5	5	-1.3	138	2.2			
HB-9S	Huangboshuwan	Quartz	9	5	-1.6	126	2.7			
			6	7	-1.4	135	2.35			
			8	5	-1.7	169	2.85			
			10	10	-2.8	195	4.6			
			6~7	15	-1.1	200	1.85			
S-26	Shuang'an	Quartz	12	15	-0.7	120	1.2			
			10	20	-1.5	160	2.55			
			10	20	-2.2	152	3.65			
After Duan 1999	?	Huangboshuwan	Witherite	5~7	5		115~160	13.6		
After Liu et al. 2010	Huangboshuwan	Quartz	5~29	3~9	-4.3	113~154	2.24~9.60			
			05hb11	Huangboshuwan	Quartz	6~20	4~12	-7.2	173~256	6.59~13.72
			05hb14-1	Huangboshuwan	Barite	5~12	3~8	-6	144~204	5.11~11.81

Notes: Tm-ice (°C) – freezing temperature; Th (°C) – homogenization temperature; Slt (wt% NaCl eq.) – salinity.

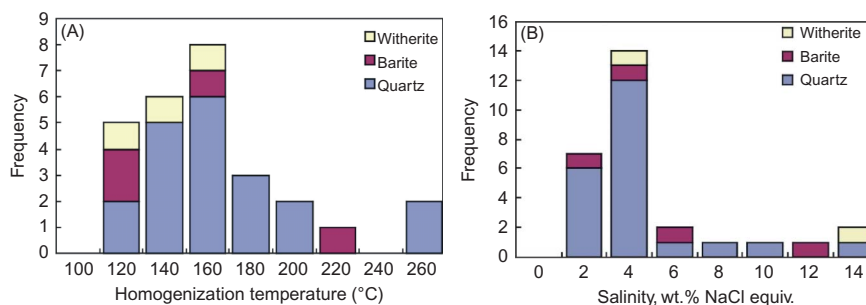


Figure 6. Histograms of (A) homogenization temperatures of fluid inclusions found in quartz, barite, and witherite from the Ziyang area, Daba region, China; (B) variations in the salinity of fluid inclusions present in the Ziyang area, Daba region, China.

less than 0.4 wt.% (Table 3), which is consistent with a hydrothermal origin (Yamamoto 1987).

Bostrom *et al.* (1979) proposed that marine sediments derived from a hydrothermal fluid have low Al/(Al+Fe+Mn) ratios. The siliceous rocks of the study area have relatively low Al/(Al+Fe+Mn) ratios (averaging 0.18) (Table 3). These values overlap with those of hydrothermal siliceous rocks from western Qinling, China (0.15) (Liu *et al.* 1999), Pingying, Shandong Province, China (0.21) (Xu *et al.* 1997), and the Franciscan and Shimanto terrains (0.21) (Yamamoto 1987). All siliceous rocks in this study fall within the fields of hydrothermal, sedimentary siliceous rocks in the Al–Fe–Mn triangle diagram (Figure 8).

The siliceous rocks of this study are further characterized by low Co/Ni ratios (averaging 0.06), high U/Th ratios (2.5–77), high Cu, As, and Sb contents (Table 4), which is typical of siliceous rocks formed from hydrothermal sedimentation (Bostrom *et al.* 1979; Marchig *et al.* 1982). In the (Cu+Co+Ni)×10–Fe–Mn diagram (Figure 9), all but one sample falls within the field for hydrothermal sedimentation from the Red Sea, as do other siliceous rocks of hydrothermal origin from west Qinling (Liu *et al.* 1999) and Dachang, Guangxi Province (Chen and Chen 1989).

Hydrothermal sediments generally have lower Zr contents (less than 50 ppm) than deep-sea sediments (Zr > 100 ppm, due to diagenesis) (Marchig *et al.* 1982). Zirconium

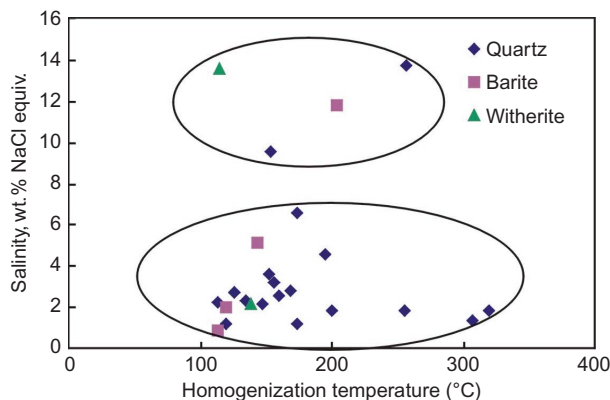


Figure 7. Plot of homogenization temperature (T_h) versus salinity for inclusions in quartz, barite, and witherite from samples collected in the Ziyang area, Daba region, China.

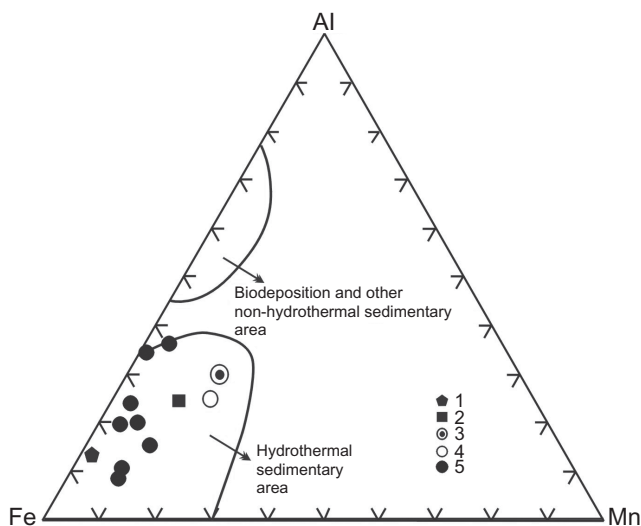


Figure 8. Al-Fe-Mn diagram for siliceous rocks of different origin(s) (after Adachi *et al.* 1986). 1, Siliceous rocks from the region of west Qinling (Liu *et al.* 1999); 2, siliceous rocks collect during the DSDP Leg 32 (Adachi *et al.* 1986); 3, cherts from the Franciscan Terrain (Yamamoto 1987); 4, cherts from the Shimanto Terrain (Yamamoto 1987); and for comparison, 5, siliceous rocks from the Ziyang study area.

contents of the siliceous rocks in this study vary from 5.35 ppm to 82.5 ppm (Table 4), with an average of 33.1 ppm. In the Zr-Cr diagram (Figure 10A), all our samples fall in the low-Zr field as for other hydrothermal siliceous rocks (Adachi *et al.* 1986; Yamamoto 1987; Liu *et al.* 1999) and modern hydrothermal sediments.

The phosphorus content generally increases with sedimentation diagenesis and hydrothermal sedimentation. The Y contents, however, only increase with the process of sedimentation diagenesis (Marchig *et al.* 1982). In the Y-P₂O₅ plot (Figure 10B), the siliceous rocks in this study, together with other hydrothermal siliceous rocks (Adachi *et al.* 1986; Yamamoto 1987; Liu *et al.* 1999), fall near the trend

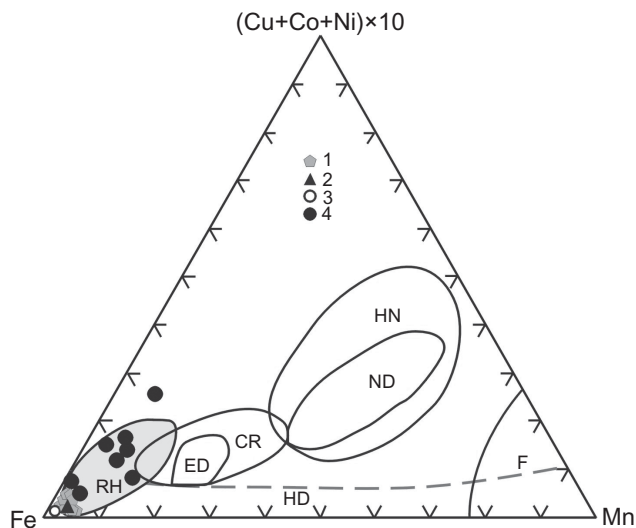


Figure 9. $(\text{Cu}+\text{Co}+\text{Ni})\times 10$ -Fe-Mn diagram for siliceous rocks of different origin(s) (modified from Rona 1978). ED, East Pacific hydrothermal metalliferous sediment; CR, hydrothermal ferromanganese crust sediment; HD, hydrothermal sedimentation area; RH, Red Sea hydrothermal sedimentation area; F, Franciscan hydrothermal sedimentation area; HN, hydrous nodule; ND, hydrous nodule. 1, Siliceous rocks from west Qinling (Liu *et al.* 1999); 2, colloform siliceous rocks occurring at Dachang, Guangxi (Chen and Chen 1989); 3, exhalative sedimentary siliceous rocks from Dachang, Guangxi (Chen and Chen 1989); and 4, siliceous rocks of the study area.

of modern hydrothermal sediments or within the area outlined for hydrothermal-type metalliferous sediments (HD), but are far away from the fields of deep-sea sediments and diagenetic-type metalliferous sediments.

Rare earth element (REE) composition is an important indicator used to distinguish hydrothermal sediments from those of a non-hydrothermal origin (Marchig *et al.* 1982; Wang *et al.* 1989). Generally, hydrothermal, sedimentary siliceous rocks are characterized by low total REE (ΣREE), remarkable Ce-negative anomalies, and weakly negative to positive Eu anomalies (Shimizu and Masuda 1977; Rona 1978; Marchig *et al.* 1982; Fleet 1983; Pan *et al.* 2001; Qi *et al.* 2003). The C1-chondrite-normalized REE patterns of the siliceous rocks in this study display the right-inclined type ($\text{La}_N/\text{Yb}_N = 1.64\text{--}35.7$) with moderate to small negative Ce anomalies (Figure 3), again typical of hydrothermal origin siliceous rocks (Zhou 1993).

The maximum reported value for $\delta^{30}\text{Si}$ is 1.4‰ for quartz formed at low temperatures in groundwater; the $\delta^{30}\text{Si}$ values of siliceous rocks from hydrothermal sedimentation range from -1.5‰ to 0.8‰; and the $\delta^{30}\text{Si}$ values of lithogenetic quartz vary between -0.2‰ and 0.3‰ (Douthitt 1982; Clayton 1986; Song and Ding 1989; Ding 1990). As such, the $\delta^{30}\text{Si}$ values of the siliceous rocks in this study (-0.3‰ to 0.6‰) are similar to those of siliceous rocks from hydrothermal sedimentation (-1.5‰ to 0.8‰) and differ from quartz formed in groundwater (Figure 4A).

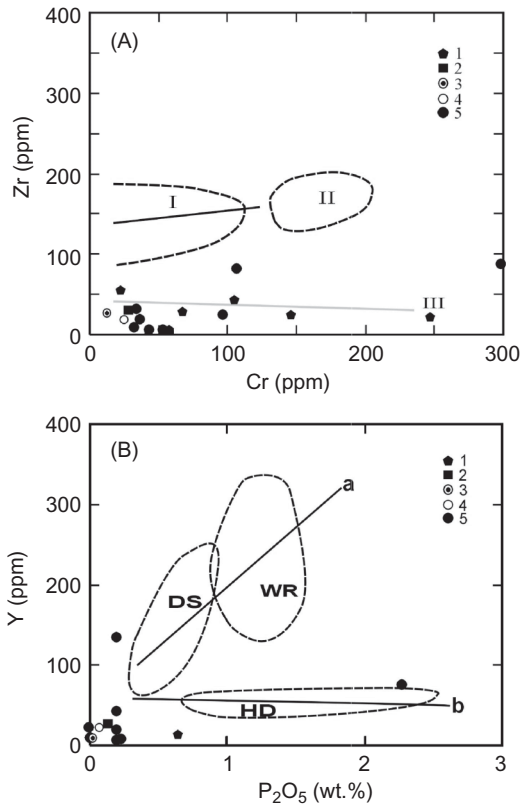


Figure 10. (A) Zr versus Cr diagram for modern sediments (after Marchig *et al.* 1982). I, Trend line for modern hydrothermal sediments and their area of concentration; II, distribution area of modern hydrothermal-diagenetic metalliferous sediments; III, trend for modern hydrothermal sediments; and samples: 1, West Qiling siliceous rock (Liu *et al.* 1999); 2, DSDP Leg 32 chert (Adachi *et al.* 1986); 3, chert from the Franciscan Terrain (Yamamoto 1987); 4, chert from the Shimanto Terrain (Yamamoto 1987); 5, siliceous rocks from the study area. (B) P₂O₅ (wt.%) versus Y (ppm) diagram for different types of sediments (after Marchig *et al.* 1982). a, trend line for modern hydrothermal sediments; b, trend line for modern hydrothermal sediments; DS, field of deep-sea sediments; WR, field for diagenetic-type metalliferous sediments; and HD, field for hydrothermal-type metalliferous sediments. Other sample numbers as for (A).

Further, they are comparable to those of the hydrothermal siliceous rocks from Dachang (0.4‰ to 0.6‰), Guangxi, China (Han and Shen 1994), and Early Cambrian siliceous rocks from Quruqtagh (−1.1‰ to 0.8‰), Xinjiang, Western China (Yang *et al.* 2006). The $\delta^{18}\text{O}$ values of our samples (16.1‰ to 21.7‰) overlap with those of quartz from hot springs (12.2‰ to 23.6‰) and also to diagenetic quartz (13‰ to 36‰) (Clayton 1986), but are different from those of igneous quartz (8.3‰ to 11.2‰) and metamorphic quartz (11.2‰ to 16.4‰) (Figure 4B).

Sedimentary environment

The Ziyang Se-enrichment areas as studied in this article are located near the Hongchunba-Zengjiaba Fault in

the Caledonian fold belt of the North Daba Mountains (Li *et al.* 1982; 2000; Mei 1985; Luo *et al.* 2001, 2004). Hydrothermal siliceous rocks appear to be preferentially formed in extensional, rift-type environments or fault-controlled basins, and tend to be associated with large-scale syn-sedimentary faults. For example, the La'erma-Qiongmo Se deposit in western Qinling is located on the Bailongjiang Great Fault (Liu *et al.* 2000).

The Lower Cambrian 'black rock series' lithologies in the Yangtze Platform (e.g. eastern Yunnan, Hunan, Guizhou, Sichuan, and Southern Shaanxi province) comprise carbonate, black shale, stone-coal, siliceous shale, chert, carbonaceous siliceous rock, and carbonaceous slate (Fan 1983; Fan *et al.* 1984; Steiner *et al.* 2001; Mao *et al.* 2002; Jiang *et al.* 2006; Orberger *et al.* 2007; Feng *et al.* 2010). During the Early Cambrian period, there were four kinds of strata containing stone-coal in southern China: the Nanling, Yangtze, Jiangnan, and Huanan types, and each coal differs in terms of quality and quantity among these. Based on the work of Jiang *et al.* (1994) these differences are mainly related to sedimentary environment (e.g. shallow-water platform, deep-water basin, and deep-water continental slope). Rocks of the Ziyang study area are interpreted as belonging to the Nanling-type strata and, as such, sedimentation is unlikely to have occurred in an abyssal-type of environment, considering the presence of carbonates. On the other hand, the absence of coarse-grained sediments within the sequence would appear to exclude a shallow marine environment. Owing to a rise in global sea levels and nutrition-abundant sea water carried into the area by upwelling, a bloom of microorganisms can be envisaged to have occurred during conditions of low sedimentation, which resulted in an oxygen-deficient environment close to the sea floor. Accordingly, the siliceous rocks with stone-coal strata in the study area are considered to have formed in a semi-deep sea sedimentary environment (such as a deep-water continental slope or continental rise).

Selenium enrichment in Lower Cambrian siliceous rocks is not limited to just the Ziyang study area. Anomalous concentrations of Se, together with Cu, Pb, Zn, As, Sb, S, Ni, V, Mn, Mo, U, Ag, Au, and PGE, have been recognized in the Lower Cambrian 'black rock series' in many parts of the Yangtze and Tarim cratons of southern and western China (Fan 1983; Fan *et al.* 1984; Chen 1990; Li and Gao, 1996, 2000; Steiner *et al.* 2001; Mao *et al.* 2002; Jiang *et al.* 2003, 2006, 2007; Orberger *et al.* 2007). This anomalous elemental association and their concentration within a limited stratigraphic interval, that occurs over a wide area, suggests that the enrichment processes may have been controlled by factors external to the crust and/or the sedimentary basins. The recognition of a hydrothermal origin for the siliceous rocks of the Ziyang study area supports the proposal that Se and other elements, that tend to be associated with mafic and

ultramafic rocks (especially Ni, V, and PGE), were probably, ultimately derived from deep-seated (i.e. magmatic) sources.

Conclusions

Our new geochemical studies of various types of siliceous rocks present in Lower Cambrian Lujiaping Formation in the Ziyang area indicate that primarily carbonaceous siliciclastic varieties are the dominant Se-bearing hosts in the Daba area. Major, trace elements, and Si and O isotopic bulk-rock analyses, furthermore, indicate that the siliceous rocks were derived as the result of hydrothermal sedimentation in a relatively anoxic semi-deep sea, sedimentary environment. The aqueous fluid responsible for mineralization was the mixing product of low-temperature high-salinity fluid, low-temperature low-salinity fluid, and high-temperature low-salinity basinal fluids in the NaCl–(KCl)–H₂O system.

Acknowledgements

This work was financially supported by National Natural Science Foundation of China (Grant No. 40972071, 40773020) and Science and Technology Foundation of Guizhou Province, China (Grant No. 2008 [2015]).

References

- Adachi, M., Yamamoto, K., and Suigiski, R., 1986, Hydrothermal chert and associated siliceous rocks from the Northern Pacific: Their geological significance as indication of Ocean Ridge Activity: *Sedimentary Geology*, v. 47, p. 125–148.
- Bostrom, K., Rydell, H., and Joensuu, O., 1979, Langbank: An exhalative sedimentary deposit: *Economic Geology*, v. 74, p. 1002–1011.
- Bureau of Geology and Mineral Resources of Shaanxi Province (BGMRs), 1982, Ministry of Geology and Mineral Resources of the People's Republic of China. *Geological Memoirs*, Series 1, no. 13: Beijing, Geological Publishing House, p. 76–302 (in Chinese).
- Chen, N.S., 1990, Lower Cambrian black shale series and associated stratiform deposits in southwest China: *Chinese Journal of Geochemistry*, v. 9, p. 244–255.
- Chen, X.P., and Chen, D.F., 1989, The hydrothermal sedimentary geochemical characteristic of Upper Devonian breast-shaped cherts in Guangxi: *Geochimica*, v. 1, p. 1–8 (in Chinese with English abstract).
- Chi, G.X., and Ni, P., 2007, Equations for calculation of NaCl/(NaCl+CaCl₂) ratios and salinities from hydrohalite-melting and ice-melting temperatures in the H₂O–NaCl–CaCl₂ system: *Acta Petrologica Sinica*, v. 23, p. 33–37.
- Clayton, R.N., 1986, High temperature isotope effects in the early solar system, *in* Valley, et al., ed., *Reviews in Mineralogy*, v. 16, p. 129–139.
- Clayton, R.N., and Mayeda, T.K., 1963, The use of bromine pentafluoride in the extraction of oxygen from oxides and silicates for isotopic analysis: *Geochimica et Cosmochimica Acta*, v. 27, p. 43–52.
- Coveney, R.M., Jr., Murowchick, J.B., Grauch, R.I., Chen, N., Glascock, M.D., and Denison, J.R., 1992, Gold and platinum in shales with evidence against extraterrestrial sources of metals: *Chemical Geology*, v. 99, p. 101–104.
- Coveney, R.M. Jr., Grauch, R.I., and Murowchick, J.B., 1994, Metals, phosphate and stone coal in the Proterozoic and Cambrian of China; the geologic setting of precious metal-bearing Ni–Mo ore beds: *Society for Economic Geology Newsletter*, v. 18, p. 1–11.
- D'yachkova, I.B., and Khodakovskiy, I.L., 1968, Thermodynamic equilibria in the systems S–H₂O, Se–H₂O, and Te–H₂O in the 25–300°C temperature range and their geochemical interpretations: *International Geochemistry*, v. 5, p. 1108–1125.
- Ding, T.P., 1990, Advances in silicon isotope geochemistry: *Journal of Mineralogy, Petrology and Geochemistry*, v. 3, p. 99–101 (in Chinese with English abstract).
- Douthitt, C.B., 1982, The geochemistry of the stable isotopes of silicon: *Geochimica et Cosmochimica Acta*, v. 46, p. 1449–1458.
- Duan, M.H.S., 1999, The geological feature of Sinian witherite mineralized belt in Zhenba-Chenkou: *Journal of Xi'an Mining Institute*, v. 19, p. 329–332 (in Chinese with English abstract).
- Edmond, J.M., and Damm, K.V., 1983, Hot spring at the seafloor: *Science*, v. 8, p. 37–50.
- Fan, D.L., 1983, Polyelements in the Lower Cambrian black shale series in southern China, *in* Augustithis, S.S., ed., *The significance of trace metals in solving petrogenetic problems and controversies*: Athens, The Ophrastus Publication, p. 447–474.
- Fan, D.L., Yang, R.D., and Huang, Z.X., 1984, The Lower Cambrian black shale series and iridium anomaly in South China, *in* Development in Geoscience, Contributions to the 27th International Geological Congress, Moscow: Beijing, Science Press, p. 215–224.
- Feng, C.X., 2004, The enriching-mechanism of selenium of Cambrian and Permian silicalite formation in the peripheral margins of Yangtze Block-taking Yutangba and Ziyang selenium-rich areas as an example [Ph.D. dissertation]: Guiyang, Guizhou Province, China, Institute of Geochemistry, Chinese Academy of Sciences (in Chinese with English abstract).
- Feng, C.X., and Liu, J.J., 2001, The research status and mineralization significance of cherts: *World Geology*, v. 20, p. 119–123 (in Chinese with English abstract).
- Feng, C.X., Liu, J.J., Hu, R.Z., and Liu, S., 2004, Geochemistry of the Yutangba Se Deposit in Western Hubei, China: *Chinese Journal of Geochemistry*, v. 23, p. 255–264.
- Feng, C.X., Liu, J.J., Hu, R.Z., and Liu, S., 2007a, Geochemical characteristics of selenium-rich silicalite formation in Ziyang, Southern Qinling, China: *Geochimica et Cosmochimica Acta*, v. 71, p. 271.
- Feng, C.X., Liu, J.J., Hu, R.Z., and Liu, S., 2007b, Introduction of Yutangba Selenium deposit in Enshi, China, *Annual meeting of Korea Society of Economic and Environmental Geology*, p. 20.
- Feng, C.X., Liu, J.J., Liu, S., Li, Z.M., and Li, E.D., 2002, The geochemistry and genesis of siliceous rocks of selenium diggings in Yutangba: *Acta Sedimentologica Sinica*, v. 20, p. 727–732 (in Chinese with English abstract).
- Feng, C.X., Liu, S., Hu, R.Z., Liu, J.J., Luo, T.Y., Chi, G.X., and Qi, Y.Q., 2010, Geochemistry of Lower Cambrian Se-rich black rock series in Guizhou Province, southwest of China: The petrogenesis and enrichment mechanism of selenium: *Earth Science-Journal of China University of Geosciences*, v. 35, p. 947–958 (in Chinese with English abstract).

- Fleet, A.J., 1983, Hydrothermal and hydrogenous ferromanganese deposits, in Rona, P.A. et al., eds., Hydrothermal process at sea floor spreading centres: Amsterdam, Elsevier Science Publishers B.V., p. 537–570.
- Förster, H.J., and Tischendorf, G., 2001, Se-rich tennantite and constraints on P-T-X conditions of selenide mineral formation in the Schlemma-Alberoda uranium ore district (western Erzgebirge, Germany): Neues Jahrbuch Fur Mineralogie. Abhandlungen, v. 176, p. 109–126.
- Grauch, R., Gent, C.A., Goldhaber, M.B., and Coveney, R.M., 1991, Cyclic sea floor exhalation, diagenesis, and turbidity flow in the formation of polymetallic (Ni–Mo–PGE) deposits in black shales: An example from Canada: Geological Society of America, Program with abstract, p. A171.
- Han, F., and Shen, J.Z., 1994, Silicon and oxygen stable isotope geochemistry of Dachang tin deposit: Acta Mineralogical Sinica, v. 14, p. 172–180 (in Chinese with English abstract).
- Hulbert, L.J., Carne, R.C., Gregoire, D.C., and Paktunc, D., 1992, Sedimentary Ni, Zn, and platinum group element mineralization in Devonian black shales, Nick Basin, Yukon, Canada: A new environment and deposit type: Exploration and Mining Geology, v. 21, p. 39–62.
- Jiang, S.Y., Chen, Y.Q., Ling, H.F., Yang, J.H., Feng, H.Z., and Ni, P., 2006, Trace and rare-earth element geochemistry and Pb–Pb dating of black shales and intercalated Ni–Mo–PGE–Au sulfide ores in Lower Cambrian strata, Yangtze Platform, South China: Mineralium Deposita, v. 41, p. 453–467.
- Jiang, S.Y., Yang, J.H., Ling, H.F., Chen, Y.Q., Feng, H.Z., Zhao, K.D., and Ni, P., 2007, Extreme enrichment of polymetallic Ni–Mo–PGE–Au in Lower Cambrian black shales of South China: an Os isotope and PGE geochemical investigation: Palaeo, v. 251, p. 217–228.
- Jiang, S.Y., Yang, J.H., Ling, H.F., Feng, H.Z., Chen, Y.Q., Chen, J.H., 2003, Re–Os isotopes and PGE geochemistry of black shales and intercalated Ni–Mo polymetallic sulfide bed from the Lower Cambrian Niutitang Formation, South China: Progress Nature Science, v. 13, p. 788–794.
- Jiang, Y.H., Yue, W.Z., and Ye, Z.Z., 1994, Characteristics, sedimentary environment and origin of the Lower Cambrian stone-like coal in southern China: Coal Geology of China (in Chinese with English abstracts), v. 6, p. 26–31.
- Kirst, L.R., and Timo, H., 1996, Geochemistry and genesis of the black shale-hosted Ni–Cu–Zn deposit at Talvivaara, Finland: Economic Geology, v. 91, p. 80–110.
- Kucha, H., and Pawlowski, M., 1986, Two-brine model on the genesis of stratabound Zechstein deposits (Kupferschiefer type) Poland: Mineralium Deposita, v. 21, p. 70–80.
- Li, J.X., Zhang, G.D., Ge, X.L., Zhang, Q.L., Luo, D.H., Appleton, J.D., Johnson, C.C., and Fordyce, F.M., 2000, Prediction and geochemical environmental character of human selenium imbalances: Beijing, The Geological Publishing House, p. 20–30 (in Chinese).
- Li, J.Y., Ren, S.X., and Chen, D.Z., 1982, Research on selenium in the environment and its relation with Kashin Beck disease, Shanxi Province: Journal of Environmental Sciences, v. 2, p. 91–100 (in Chinese with English abstract).
- Li, S.R., and Gao, Z.M., 1996, Silicalites of hydrothermal origin in the Lower Cambrian black rock series of south China: Chinese Journal of Geochemistry, v. 15, p. 113–120.
- Li, S.R., and Gao, Z.M., 2000, Source tracing of noble metal elements in Lower Cambrian black rock series of Guizhou-Hunan Province, China: Science in China (Series D), v. 43, p. 625–632.
- Li, T., 1992, The statistical characteristics of the abundance of chemical elements in the Earth's crust: Geology and Prospecting, v. 28, p. 1–7 (in Chinese with English abstract).
- Li, Y.H., Ding, T.P., and Wan, D.F., 1995, Experimental study of silicon isotope dynamic fractionation and its application in geology: Chinese Journal of Geochemistry, v. 14, p. 212–219.
- Liu, J.J., Wu, S.H., Liu, Z.J., Su, W.C., and Wang, J.P., 2010, A discussion on the origin of witherite deposit in large scale barium metallogenic belt, southern Qinling Mountains, China: Evidence from individual fluid inclusion: Earth Science Frontiers, v. 2, p. 222–238 (in Chinese with English abstract).
- Liu, J.J., Zheng, M.H., Liu, J.M., and Su, W.C., 2000, Geochemistry of the La'erma and Qiongmo Au–Se deposits in western Qinling Mountains, China: Ore Geology Review, v. 17, p. 91–111.
- Liu, J.J., Zheng, M.H., Liu, J.M., Zhou, Y.F., Gu, X.X., and Zhang, B., 1999, The geological and geochemical characteristics of Cambrian chert and their sedimentary environmental implications in western Qinling: Acta Petrologica Sinica, v. 15, p. 145–154 (in Chinese with English abstract).
- Liu, Y.J., Cao, L.M., Li, Z.L., Wang, H.N., Chu, T.Q., and Zhang, J.R., 1984, Element geochemistry: Beijing, Science Press, p. 1–281 (in Chinese).
- Luo, K.L., and Jiang, J.S., 1995, The content and enrichment rule of selenium in the Lower Cambrian strata, Ziyang, Shanxi province: Geology and Geochemistry (in Chinese), v. 1, p. 68–71.
- Luo, K.L., Pan, Y.T., Wang, W.Y., and Tan, J.A., 2001, Selenium contents and distribution patterns in the Palaeozoic strata in southern Qinling Mountains: Geological Review, v. 47, p. 211–217 (in Chinese with English abstract).
- Luo, K.L., Xu, L.R., Tan, J.A., Wang, D.H., and Xiang, L.H., 2004, Selenium source in the selenosis area of the Daba region, South Qinling Mountain, China: Environmental Geology, v. 45, p. 426–432.
- Luo, K.L., 2006, The Lujiaping formation of Northern Daba Mountain: Journal of Stratigraphy, v. 30, p. 149–156 (in Chinese with English abstract).
- Mao, J.W., Lehmann, B., Du, A.D., Zhang, G.D., Ma, D.S., Wang, Y.T., Zeng, M.G., and Kerrich, R., 2002, Re–Os dating of polymetallic Ni–Mo–PGE–Au mineralization in Lower Cambrian Black Shales and its geologic significance: Economic Geology, v. 47, p. 1051–1061.
- Marchig, V., Gundlach, H., and Moller, P., 1982, Some geochemical indication for determination between diagenetic and hydrothermal metalliferous sediments: Marine Geology, v. 50, p. 241–256.
- Mei, Z.Q., 1985, A review on the two selenium areas so far discovered in China: Chinese Journal of Endemic Diseases, v. 4, p. 379–385 (in Chinese).
- Mossman, D., Gauthier-Lafaye, F., and Jackson, S.E., 2005, Black shales, organic matter, ore genesis and hydrocarbon generation on the Paleoproterozoic Franceville Series, Gabon: Precambrian Research, v. 137, p. 253–272.
- Orberger, B., Vymazalova, A., Wagner, C., Fialin, M., Gallien, J.P., Wirth, R., Pasava, J., and Montagnac, G., 2007, Biogenic origin of intergrown Mo–sulphide–and carbonaceous matter in Lower Cambrian black shales (Zunyi Formation, southern China): Chemical Geology, v. 238, p. 213–231.
- Pan, J.Y., Zhang, Q., Ma, D.S., and Li, C.Y., 2001, Cherts from the Yangla copper deposit, western Yunnan Province: Geochemical characteristics and relationship with massive sulfide mineralization: Science in China (Series D), v. 31, p. 10–16 (in Chinese).
- Pasava, J., 1993, Anoxic sediments—an important environment for PGE; an overview: Ore Geology Review, v. 8, p. 425–445.

- Polgáry, M., Tazaki, K., Watanabe, H., Vigh, T., and Gucsik, A., 2006, Geochemical aspect of chemolithoautotrophic bacterial activity in the role of black shale hosted Mn mineralisation, Jurassic age, Hungary, Europe: *Clay Science*, v. 12, p. 233–239.
- Püttmann, W., Hagemann, H.W., Merz, C., and Speczik, S., 1988, Influence of organic matter in transport and accumulation of metals exemplified at the Permian Kupferschiefer formation: *Ore Geology Review*, v. 6, p. 563–579.
- Qi, H.W., Hu, R.Z., Su, W.C., Qi, L., and Feng, J.Y., 2003, Siliceous rocks of terrestrial hydrothermal sedimentation origin and the genesis of super-large germanium deposits as exemplified by the Lingcang germanium deposit: *Science in China (Series D)*, v. 33, p. 236–246 (in Chinese).
- Qi, L., Hu, J., and Gregoire, D.C., 2000, Determination of trace elements in granite by inductively coupled plasma mass spectrometry: *Talanta*, v. 51, p. 507–513.
- Roedder, E., 1984, Fluid inclusions (Rev Mineral 12): Mineralogical Society of America, p. 644.
- Rona, P.A., 1978, Criteria for recognition of hydrothermal mineral deposits in ocean crust: *Economic Geology*, v. 73, p. 135–160.
- Sawlowicz, Z., 1989, Isotopic composition of C, O, S in the organic rich copper-bearing shales from the Kupferschiefer in Poland: *Arch. Miner.*, v. 44, p. 5–19.
- Shepherd, T.J., Ranking, A.H., and Alderthon, D.H.M., 1985, A practical guide to fluid inclusion studies: Glasgow and London, Blackie and Son, p. 239.
- Shimizu, H., and Masuda, A., 1977, Cerium in chert as an indication of marine environment of its formation: *Nature*, v. 266, p. 346–348.
- Simon, G., and Essene, E.J., 1996, Phase relation among selenides, sulfides, tellurides, and oxides: Thermodynamic data and calculated equilibria: *Economic Geology*, v. 91, p. 1183–1208.
- Simon, G., Kesler, S.E., and Essene, E.J., 1997, Phase relation among selenides, sulfides, tellurides and oxides: Application to selenide-bearing ore deposits: *Economic Geology*, v. 92, p. 468–484.
- Song, C.Z., 1989, A brief description of the Yutangba sedimentary-type selenium mineralized area in southwestern Hubei: *Mineral Deposits*, v. 8, p. 83–89 (in Chinese with English abstract).
- Song, T.R., and Ding, T.P., 1989, The trial application of silicon isotopes ($\delta^{30}\text{Si}$) in siliceous rocks to sedimentary facies analysis: *Chinese Science Bulletin*, v. 34, p. 1408–1411 (in Chinese with English abstract).
- Steiner, M., Wallis, E., Erdtmann, B.D., Zhao, Y.L., and Yang, R.D., 2001, Submarine-hydrothermal exhalative ore layers in black shales from South China and associated fossils-insights into a Lower Cambrian facies and bio-evolution: *Palaeogeography, Palaeoclimatology, and Palaeoecology*, v. 169, p. 165–191.
- Sun, S.S., and McDonough, W.F., 1989, Chemical and isotopic systematics of oceanic basalts: Implications for mantle composition and processes, in Saunders, A.D., Norry, M.J., eds., *Magmatism in the Ocean Basins*, Geological Society Special Publication, London, no. 42, p. 313–345.
- Sun, Y., and Püttmann, W., 1997, Metal accumulation during and after deposition of the Kupferschiefer from Sangerhausen Basin, Germany: *Applied Geochemistry*, v. 12, p. 577–592.
- Wang, H.F., and Li, J.Q., 1996, The geological characteristic of Se-deposit in Shuanghe, Enshi, Hubei Province: *Hubei Geology*, v. 10, p. 10–21 (in Chinese with English abstract).
- Wang, Z.G., Yu, X.Y., and Zhao, Z.H., 1989, The geochemistry of REE: Beijing, Science Press (in Chinese).
- Wen, H.J., 1999, A preliminary analysis of organic mineralization of the disperse element selenium: *Acta Geoscientia Sinica-Bulletin of the Chinese Academy of Geological Sciences*, v. 20, p. 190–194 (in Chinese with English abstract).
- Wen, H.J., and Qiu, Y.Z., 1999, Organic and inorganic occurrence of selenium in La'erma Se-Au deposit: *Science in China (Series D)*, v. 29, p. 426–432.
- Xu, Y.T., Zhou, B.H., and Huang, F.S., 1997, The geochemical characteristics of Middle Proterozoic hydrothermal sediments-layered silicalites and their sedimentary environment implications in Pinyin, Shandong Province: *Journal of Peking University*, v. 33, p. 167–174 (in Chinese with English abstract).
- Yamamoto, K., 1987, Geochemical characteristics and depositional environment of cherts and associated rocks in the Franciscan and Shiment terranes: *Sedimentary Geology*, v. 52, p. 65–108.
- Yang, R.D., Zhang, C.L., Luo, X.R., Tian, J.Q., Bao, Y.F., and Song, G.Q., 2006, Geochemical characteristic of Early Cambrian cherts in Quruqtagh, Xinjiang, West China: *Acta Geological Sinica*, v. 80, p. 598–605 (in Chinese with English abstract).
- Yao, L.B., Gao, Z.M., Yang, Z.S., and Long, H.B., 2002, Origin of seleniferous cherts in Yutangba Se deposit, Southwest Enshi, Hubei Province: *Science in China (Series D)*, v. 45, p. 741–854.
- Yu, B.S., and Qiu, Y.Z., 1998, The geochemistry of sedimentary rocks and its relation to crustal evolution in the southwest Yangtze Massif: *Chinese Journal of Geochemistry*, v. 17, p. 265–274.
- Yu, B.S., Chen, J.Q., Li, X.W., and Lin, C.S., 2002, Geochemistry of black shale and its significance of lithosphere evolution in the Lower Cambrian in Tarim Basin: *Science in China (Series D)*, v. 32, p. 374–382.
- Yu, B.S., Dong, H.L., Widom, E., Chen, J.Q., and Lin, C.S., 2009, Geochemistry of basal Cambrian black shales and cherts from the Northern Tarim Basin, Northwest China: Implications for depositional setting and tectonic history: *Journal of Asian Earth Sciences*, v. 34, p. 418–436.
- Zhao, C.Y., Ren, J.H., and Xue, C.Z., 1993, Selenium in soils of selenium rich areas in Ziyang County: *Acta Petrologica Sinica*, v. 30, p. 253–259 (in Chinese).
- Zhou, Y.Z., 1993, *Geology and geochemistry of Hetai gold field, southern China*: Guangzhou, South China University of Technology Press, p. 53–107 (in Chinese).
- Zhu, J.M., 2000, Modes of occurrence of Se in the black Se-rich rocks of Yutangba and its impact on the local environment (in Chinese) [Ph.D. dissertation]: Guiyang, Guizhou Province, China, Institute of geochemistry, Chinese Academy of Sciences (in Chinese with English abstract).